Navigation of UAVs for Tracking of Atmospheric Release of Radiation

Václav Šmídl, Radek Hofman

Abstract— **Navigation of unmanned aerial vehicles (UAVs) is a popular and well studied topic. In this contribution, we apply the existing decision theory to the problem of tracking atmospheric pollution, specifically accidental release of radiation. The UAVs work in tandem with the stationary radiation monitoring network to estimate consequences of the radiation accident. Results of this estimation serve as supporting material for the human decision makers, whose main concern is protection of the population. We test navigation of the UAVs with respect to two loss functions: mutual information and expected misclassification of affected people. Several approximations were designed to navigate the UAVs in real time. The simulation experiments confirm that UAVs have great potential to complement limited capabilities of the stationary radiation monitoring network.**

I. INTRODUCTION

Radioactive material is released into the atmosphere only in the case of severe accident in a nuclear power plant. It is an extremely rare event, however with severe consequences for potentially many people living in proximity of the power plant. Awareness of radiation security has been increased after the Chernobyl accident, and every country is now equipped with radiation monitoring network (RMN) of on-line connected receptors continually measuring radiation levels. With growing availability of commercial UAVs, these may become very attractive complement of existing stationary RMNs. Aerial surveillance is routinely used after the accident for measuring of the radiation from deposition. In this text, we consider the use of UAVs in the early phase of an accident to track the radioactive cloud that is still moving over the terrain.

General methodologies for tracking of radioactive releases has been studied in the literature, e.g. [1], [2], without explicit navigation of the measuring devices. On the other hand, general methodologies of design of mobile sensor networks are also available [3], [4]. In this text, we combine the general methods of sensor networks with specific features of the radiation protection. The specifics are in the loss functions and in parametrization of the state space model.

II. DECISION THEORY FRAMEWORK

Navigation of the UAVs will be formalized as a task of decision making under uncertainty. The action variable is the navigation command for every single UAV in terms of GPS coordinates. We assume that the UAV is capable

V. Smidl and R. Hofman are with the Institute of Information Theory and Automation, Prague, Czech Republic. Email: `smidl@utia.cas.cz`

of reaching the GPS position by its own means. The GPS coordinates will be assigned in a centralized way by the emergency coordination center.

The decision that is to be made at each time t is to choose the location where all UAVs should be at time $t + 1$. We assume that J UAVs are already in the air, and the action variable is a vector $\mathbf{a}_{t+1} = [\mathbf{a}_{1,t+1}, \mathbf{a}_{J,t+1}]$, from a set of possible locations $\mathcal{A}_{t+1}$. The optimal action, $\mathbf{a}_{t+1}^*$, is the one that minimizes the expected value of a chosen loss function [5]:

$$\mathbf{a}_{t+1}^* = \arg \min_{\mathbf{a}_{t+1} \in \mathcal{A}_{t+1}} \mathsf{E}(\mathcal{L}(\mathbf{x}_{t:t+h}, \mathbf{a}_{t+1:t+h})|\mathbf{y}_{1:t}), \quad (1)$$

where $\mathbf{x}_{t:t+h} = [\mathbf{x}_t, \ldots, \mathbf{x}_{t+h}]$ is the uncertain future trajectory of the state of the system, $\mathcal{L}(\mathbf{x}, \mathbf{a})$ is the loss function mapping the space of all actions and states to the real axis, $\mathbf{y}_{1:t}$ are the measured data, $\mathsf{E}(\cdot)$ is the operator of expected value with respect to probability density function $p(\cdot)$ of the random variable in argument of the expectation.

This formalism is rather general and its results will differ with different choices of the loss function $\mathcal{L}$ and/or different representations of uncertainty. Indeed, many existing solutions may be interpreted as various choices of these two factors. For example, entropy minimization techniques choose logarithm of the probability density function to be their loss function. In particular, [6] considered $\mathbf{x}_t$ to be spatial distribution of the pollutant with Gaussian distributed density and entropy of $\mathbf{x}_t$ being the loss function; [4] designed a particle filtering approximation for mutual information loss function, and [1] introduced a custom loss function for the purpose of radiation protection. We combine these approaches to design navigation strategy for the UAVs.

A. Atmospheric dispersion model

When the pollutant is released into the atmosphere, it forms a plume which is subject to wind and dispersion. For a perfectly known parameters of the release θ and a perfectly known weather conditions (containing wind speed and direction, Pasquill's stability category, etc.), the shape of the plume can be very well approximated by the Gaussian plume model or a sequence of puff models [7]. The proposed methodology will work with any type of dispersion model, however, we choose the classical *puff model* for our experiments. The puff model is formed by a sequence of puffs labeled $i = 1, \ldots, I$, each puff is assumed to approximate short period of the release be an instantaneous release of the pollutant at discrete time
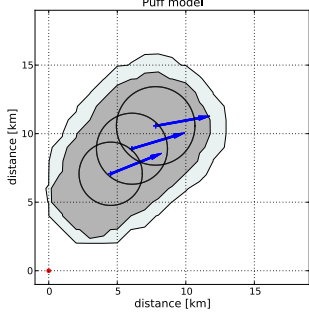
Fig. 1. Illustration of composition of the puff model for release of 6 puffs. Contours denote levels of the radiation dose $q(\mathbf{s})$ and every second puff is displayed as a circle with diameter 3σ. Current wind field is illustrated by arrows in the center of each puff.

t_i. Concentration of the pollutant in a single puff at time τ is given by:

$$C_i(\mathbf{s}, \tau) = \frac{Q_i}{(2\pi)^{3/2}\sigma_1\sigma_2\sigma_3} \exp\left[-\frac{(s_1 - l_{1,i,\tau})^2}{2\sigma_1^2}\right.$$
$$\left. -\frac{(s_2 - l_{2,i,\tau})^2}{2\sigma_2^2} - \frac{(s_3 - l_{3,i,\tau})^2}{2\sigma_3^2}\right] \quad (2)$$

where $\mathbf{s}$ is a vector of spatial coefficients, $\mathbf{l}_{i,\tau} = [l_{1,i,\tau}, l_{2,i,\tau}, l_{3,i,\tau}]$ is the vector of location of the puff center, $\sigma_1, \sigma_2, \sigma_3$ are dispersion coefficients, and Q_i is the released activity in the ith puff.

Illustration of the pollution model is displayed in Fig. 1. Spatial distribution of the pollutant is then fully determined by state variables:

$$\mathbf{x}_{pm,t} = [\mathbf{l}_{1,t} \ldots \mathbf{l}_{I,t}, Q_{1,t}, \ldots Q_{I,t}, \boldsymbol{\sigma}_{1,t}, \ldots \boldsymbol{\sigma}_{I,t}]. \quad (3)$$

Radioactive material dispersed in the plume emits ionizing radiation which can be measured, typically by the integrated mono-energetic gamma dose-rate measurements over the measurement period (typically 10min). The expected value of the measured total dose on a receptor at location $\mathbf{s}_m$ is a sum of contributions from each puff in the puff model:

$$q_t(\mathbf{s}_m) = \sum_{i=1}^{I} c_{i,t}(\mathbf{s}_m), \quad (4)$$

where the coefficient $c_{i,t}(\mathbf{s}_m)$ is computed as [8]:

$$c_{i,t}(\mathbf{s}_m) = \rho \int_{t-1}^{t} \Phi_i(\mathbf{s}_m, \tau, E) \, d\tau. \quad (5)$$

Here, ρ is a constant depending on the released material. Fluency rate $\Phi_i(\mathbf{s}_m, E)$ from the ith puff is calculated as the following three dimensional integral over the volume of the puff:

$$\Phi_i(\mathbf{s}_m, \tau, E) = \int_{\Omega} \frac{C_i(\mathbf{s}, \tau) \, B(E, \mu r) \exp(-\mu r)}{4\pi r^2} d\mathbf{s}, \quad (6)$$

$$B(E, \mu\, r) = 1 + k\, \mu r, \quad k = \frac{\mu - \mu_a}{\mu_a}. \quad (7)$$

$$r = ||\mathbf{s}_m - \mathbf{s}||. \quad (8)$$

Ambient activity concentration $C_i(\mathbf{s}, \tau)$ is defined by (2). B is the linear build-up factor, μ and μ_a are linear and mass attenuation coefficient, respectively; $\Omega \subset \mathbb{R}^3$ is a spatial domain of integration ($\mathbf{s} \in \Omega$).

B. Probabilistic state space model

Temporal evolution of the state variable (3) is subject to many uncertainties. The key uncertainty is with the released activity $Q_i, i = 1, \ldots, I$ and the weather conditions: wind direction ϕ_t, and wind speed v_t that can vary in space and time. We have chosen to model the uncertainty in the wind field as corrections of the numerical weather prediction:

$$v_t(\mathbf{s}) = \tilde{v}_t(\mathbf{s})\theta_{v,t}, \quad (9)$$
$$\phi_t(\mathbf{s}) = \tilde{\phi}_t(\mathbf{s}) + \theta_{\phi,t} + \theta_{c,t}||\mathbf{s} - \mathbf{s}_0||^2, \quad (10)$$

where $\tilde{v}_t(\mathbf{s})$, $\tilde{\phi}_t(\mathbf{s})$ are the wind speed and wind direction predicted by the numerical model at location $\mathbf{s}$, respectively. $\mathbf{s}_0$ is the location of the meteo-station and $||\cdot||$ denotes Euclidean distance. Constants $\boldsymbol{\theta}_t = [\theta_{v,t}, \theta_{\phi,t}, \theta_{c,t}]$ are unknown biases of the numerical weather forecast model at time t. Correction of the wind field forecast is then achieved by estimation of $\theta_{v,t}, \theta_{\phi,t}$ and $\theta_{c,t}$ using random walk model on their time evolution. Given wind field (9)–(10), center of the ith puff moves deterministically according to

$$l_{1,i,t+1} = l_{1,i,t} + v_t(\mathbf{l}_{i,t})\sin(\phi_t(\mathbf{l}_{i,t})),$$
$$l_{2,i,t+1} = l_{2,i,t} + v_t(\mathbf{l}_{i,t})\cos(\phi_t(\mathbf{l}_{i,t})).$$

Dispersion coefficients $\boldsymbol{\sigma}$ are deterministic functions of total traveled distance form the source and Pasquill's stability category. Temporal evolution of the released dose is modeled by a random walk model. The full state of the system is then $\mathbf{x}_t = [\mathbf{x}_{pm,t}, \boldsymbol{\theta}_t]$.

C. Measurement models

We assume that we have measurements from three sources: (i) a stationary RMN composed of radiation dose receptors at fixed locations, $\mathbf{s}_m$, $m = 1, \ldots, M$, (ii) a meteo-station near the power plant, and (iii) UAVs in the air measuring radiation dose. The vector of observations is then composed of:

$$\mathbf{y}_t = [\overline{v}_t, \overline{\phi}_t, y_{Q,1,t}, \ldots y_{Q,M,t}, z_{1,t}, \ldots, z_{J,t}],$$

where $\overline{v}_t$ and $\overline{\phi}_t$ are the measured wind speed and wind direction at the meteo-station, $y_{Q,m,t}, m = 1. \ldots, M$ are the dose measurements from the RMN and $z_{j,t}$, $j = 1, \ldots, J$ are the dose measurements from the UAVs. The

measurements are assumed to have distributions

$$
\begin{aligned}
p(\overline{v}_t|v_t(\mathbf{s}_0)) &= \Gamma(\gamma_v^{-2}, \gamma_v^2 v_t(\mathbf{s}_0)), \\
p(\overline{\phi}_t|\phi_t(\mathbf{s}_0)) &= \mathcal{N}(\phi_t(\mathbf{s}_0), \sigma_b), \\
p(y_{Q,m,t}|\mathbf{x}_t) &= \mathcal{N}\left(q_t(\mathbf{s}_m), (\gamma_Q q_t(\mathbf{s}_m))^2\right), \quad (11) \\
p(z_{j,t}|\mathbf{x}_t, \mathbf{a}_t) &= \mathcal{N}\left(q_t(\mathbf{a}_j), (\gamma_Q q_t(\mathbf{a}_j))^2\right), \quad (12)
\end{aligned}
$$

where $q_t(\cdot)$ is given by (4), and $\sigma_b, \gamma_v, \gamma_Q$ are constants given by accuracy of the used devices. Note that the locations of the RMN sensors are stable, while the position of the UAVs is changing, and thus affecting the integration path in (5). In the simulation we assume linear interpolation of the UAVs' position between $\mathbf{a}_t$ and $\mathbf{a}_{t+1}$.

D. Loss function

We briefly review typical loss function used in the literature.

1) Entropy and mutual information: The purpose of the locating new mobile measuring station is to reduce uncertainty in the estimated parameters. This idea can be formalized using the joint entropy of the state and the observations [9], [6].

$$
H(\mathbf{x}_t, \mathbf{y}_t) = -\int p(\mathbf{x}_t, \mathbf{y}_t|I_t) \log p(\mathbf{x}_t, \mathbf{y}_t|I_t) d\mathbf{x}_t d\mathbf{y}_t \quad (13)
$$

where $I_t = \{y_{1:t-1}, \mathbf{a}_t\}$. A common assumption made e.g. in [6] is that the total entropy $H(\mathbf{x}_t, z_t)$ is constant for all locations $\mathbf{a}_t$. This is true only under the assumption that the entropy of measurements is independent of its location $\mathbf{a}_t$ and $\mathbf{x}_t$. This assumption does not hold for (11), hence we will use the mutual information loss [4]:

$$
I(\mathbf{x}_t; \mathbf{y}_t) = H(\mathbf{y}_t) + H(\mathbf{x}_t) - H(\mathbf{x}_t, \mathbf{y}_t). \quad (14)
$$

Since $H(\mathbf{x}_t)$ can not be influenced by actions $\mathbf{a}_t$, we need to evaluate (13) and

$$
H(\mathbf{y}_t) = -\int p(\mathbf{y}_t|I_t) \log p(\mathbf{y}_t|I_t) d\mathbf{y}_t. \quad (15)
$$

2) Misclassification of decision: An alternative loss function for the purpose of radiation protection is defined with respect to the final decision on the countermeasures. The countermeasures for radiation protection are defined by laws. Typically, the limits for introduction of countermeasures are given in terms of the expected total received dose

$$
d_T(\mathbf{s}_m) = \sum_{t=1}^T q_t(\mathbf{s}_m), \quad (16)
$$

where T is the time when contribution from q_t drops zero. The law gives various values of threshold, $\overline{d}$, for introduction of a specific countermeasure.

A suitable loss function for the purpose of radiation protection is defined in terms of incorrectly classified people in the considered evacuation zones [1]:

$$
L(\mathbf{x}_{t:T}, \mathbf{a}_{t:T}) = \alpha I_{fp} + \beta I_{fn}, \quad (17)
$$

where I_{fp} is the number of people incorrectly classified for evacuation, and I_{fn} is the number of people that are incorrectly classified to stay in the polluted area. We split the emergency planning zone around the power plant into K areas, each representing a constant number of inhabitants, e.g. 100, each with a predefined location, $\mathbf{i}_k$, $k = 1 \ldots K$. The total number of incorrectly classified inhabitants is then

$$
I_{fp} = \sum_{k=1}^K \mathsf{E}\left(\hat{d}(\mathbf{i}_k) > \overline{d} \,\&\, d(\mathbf{i}_k) < \overline{d}\right), \quad (18)
$$

$$
I_{fn} = \sum_{k=1}^K \mathsf{E}\left(\hat{d}(\mathbf{i}_k) < \overline{d} \,\&\, d(\mathbf{i}_k) > \overline{d}\right), \quad (19)
$$

where $\hat{d}$ is defined as a point estimate of the total dose (16)

$$
\hat{d}(\mathbf{i}_k) = \int d(\mathbf{i}_k) p(\mathbf{x}_{t:T}|\mathbf{y}_{t:T}) d\mathbf{x}_{t:T}, \quad (20)
$$

$$
p(\mathbf{x}_{t:T}|\mathbf{y}_{t:T}) \propto p(\mathbf{x}_t) \prod_{\tau=t+1}^T p(\mathbf{y}_\tau|\mathbf{x}_\tau, \mathbf{a}_\tau) p(\mathbf{x}_\tau|\mathbf{x}_{\tau-1}) \quad (21)
$$

Since future values of the observations $\mathbf{y}_{t+1:T}$ are unknown, the expectations in (18)–(19) are also over $p(\mathbf{y}_{t+1:T}|\cdot)$.

Note that optimization of (17) can not be decomposed into the common additive form due to the presence of logical expressions in (18)–(19). This would make evaluation of the loss extremely time consuming. Therefore, we propose to decompose (17) into the following approximate additive loss:

$$
L(\mathbf{x}_{t:T}, \mathbf{a}_{t:T}) \approx \sum_{t=1}^T \alpha I_{fp,t} + \beta I_{fn,t}, \quad (22)
$$

$$
I_{fp,t} = \sum_{k=1}^K \mathsf{E}\left(\hat{q}_t(\mathbf{i}_k) > \overline{q} \,\&\, q_t(\mathbf{i}_k) < \overline{q}\right),
$$

$$
I_{fn,t} = \sum_{k=1}^K \mathsf{E}\left(\hat{q}_t(\mathbf{i}_k) < \overline{q} \,\&\, q_t(\mathbf{i}_k) > \overline{q}\right).
$$

Here, $\overline{q}$ is an empirically chosen limit.

E. Particle filter estimation

We assume that all uncertainty is modeled by an empirical probability density function

$$
p(x_{1:t}|\mathbf{y}_{1:t}) \approx \sum_{n=1}^N w_t^{(n)} \delta(\mathbf{x}_{1:t} - \mathbf{x}_{1:t}^{(n)}), \quad (23)
$$

where $\mathbf{x}_{1:t}^{(n)}$, $n = 1, \ldots, N$, is a sample of the state space trajectory. Assimilation of the measured data is then achieved via sampling-importance-resampling procedure, where the weights can be computed recursively,

$$
w_t^{(n)} \propto w_{t-1}^{(n)} \frac{p(\mathbf{y}_t|\mathbf{x}_t) p(\mathbf{x}_t|\mathbf{x}_{t-1})}{q(\mathbf{x}_t|\mathbf{y}_t)}. \quad (24)
$$

Good proposal function and resampling strategy are necessary steps preventing degeneracy of the particle filter (24), [10].

III. Navigation of UAVs

A. Decision space and optimal decisions

We assume that within the sampling period, the UAVs can fly a maximum distance d_{max}. Hence, the required location $\mathbf{a}_{j,t+1}$ must satisfy $||\mathbf{a}_{j,t+1} - \mathbf{a}_{j,t}|| < d_{max}$. Hence, we discretize the space of potential actions into R points on polar coordinates within the maximum distance, see Fig. 5 for illustration. The total number of potential decisions in $\mathcal{A}_{t+1}$ for one-step-ahead optimization is then R^J.

Optimal decisions are obtained by evaluation of one-step-ahead optimization of the chosen loss function for all combinations of the potential decisions. Sampling time of the decisions is 10min. The decision is then submitted as a setpoint to the UAVs that navigate to the given coordinates autonomously.

B. Evaluation of the mutual information

For the mutual information loss (14), we are to evaluate relation (13) and (15). We assume that all measurements (11) are uncorrelated, hence the only measurements that are affected by the control action are $\mathbf{z}_t$. Under the chosen approximation (23), the joint and the marginal densities are

$$p(\mathbf{x}_t, \mathbf{z}_t | \mathbf{y}_{1:t-1}, \mathbf{a}_t) = \sum_{n=1}^{N} w_t^{(n)} p(\mathbf{z}_t | \mathbf{x}_t, \mathbf{a}_t) \delta(\mathbf{x}_t - \mathbf{x}_t^{(n)}). \tag{25}$$

$$p(\mathbf{z}_t | \mathbf{y}_{1:t-1}, \mathbf{a}_t) = \sum_{n=1}^{N} w_t^{(n)} p(\mathbf{z}_t | \mathbf{x}_t, \mathbf{a}_t). \tag{26}$$

Substituting (25) into (13)–(15) we obtain:

$$H(\mathbf{x}_t, \mathbf{z}_t) = \sum_{n=1}^{N} w_t^{(n)} H(\mathbf{z}_t | \mathbf{x}_t^{(n)}), \tag{27}$$

$$H(\mathbf{z}_t) = \sum_{n=1}^{N} w_t^{(n)} \int p(\mathbf{z}_t | \mathbf{x}_t^{(n)}, \mathbf{a}_t) \times \tag{28}$$
$$\times \log \left[\sum_{n=1}^{N} w_t^{(n)} p(\mathbf{z}_t | \mathbf{x}_t^{(n)}, \mathbf{a}_t) \right] d\mathbf{y}_t.$$

Note that evaluation of (27) for (11) is relatively simple:

$$H(\mathbf{x}_t, \mathbf{y}_t) = \sum_{n=1}^{N} w_t^{(n)} \sum_{j=1}^{J} \log \left(q_t(\mathbf{a}_j, x_t^{(n)}) \right) + c,$$

where $c = -\frac{1}{2} J \log(2\pi e) + J \log \gamma$ is constant for all $\mathbf{a}_t$. However, evaluation of (28) is a complex integral which is hard to evaluate.

Therefore, we propose to simplify its evaluation using Gaussian approximation of the mixture (25) obtained by

---

Algorithm 1 Importance sampling for evaluation of the misclassification loss.

For each particle n do
  1) generate samples of fictitious measurements $\mathbf{y}_{t+1}^{(n)}$
  2) Compute weights (24) using $\mathbf{y}_{t+1}^{(n)}$,
  3) Compute expected value $\hat{\mathbf{c}}$, and $L(\hat{C}(Z^{(k)}), X^{(n)})$,

Compute the loss function via (31).

---

moment matching:

$$p(\mathbf{z}_t | y_{1:t-1}, \mathbf{a}_t) = \mathcal{N}(\mu_y, \sigma_y), \tag{29}$$
$$\mu_y = \sum_{n=1}^{N} w_t^{(n)} q_t(\mathbf{a}_t, x_t^{(n)}),$$
$$\sigma_y = \left[\sum_{n=1}^{N} w_t^{(n)} (\gamma_Q + 1)(q_t(\mathbf{a}_t, x_t^{(n)}))^2 \right] - \mu_y^2.$$

Then, entropy (28) is approximated by the entropy of the Gaussian distribution

$$H(\mathbf{y}_t) \approx \frac{1}{2} \log \left[(2\pi e) |\sigma_y| \right]. \tag{30}$$

Suitability of the approximation with be compared to numerical integration of (15) in Section 4.

Remark: In this Section we assume mutual information of the predictive density for simplicity. More complex schemes can be designed using posterior density.

C. Evaluation of the misclassification loss

Evaluation of the misclassification loss (22) is harder than that of the mutual information, since we consider posterior estimates

$$\hat{q}_{t+1}(\mathbf{l}) = \int p(q_{t+1}(\mathbf{l}) | \mathbf{x}_{t+1}) p(\mathbf{x}_{t+1} | \mathbf{y}_{1:t+1}) d\mathbf{x}_{t+1},$$

that are functions of $\mathbf{y}_{t+1}$ and the expected value (22) is

$$I_{fn,t+1} = \sum_{n=1}^{N} \sum_{k=1}^{K} \int p(\mathbf{y}_{t+1} | \mathbf{x}_{t+1}) p(\mathbf{x}_{t+1} | \mathbf{x}_t^{(n)}) \times \tag{31}$$
$$\times (\hat{q}_t(\mathbf{i}_k) < \bar{q} \,\&\, q_t(\mathbf{i}_k) > \bar{q}) \, d\mathbf{x}_{t+1} d\mathbf{y}_{t+1}.$$

Similarly to (28), integration in (31) needs to be approximated.

Since (22) is an expected value, we may use the importance sampling procedure to draw N samples of $\mathbf{x}_{t+1}, \mathbf{y}_{t+1}$ and approximate (31) by summation. In effect, this algorithm works as generation of fictitious measurements $\mathbf{y}_{t+1}$ and application of the particle filter to these measurements. The algorithm is summarized in Algorithm 1.

In principle, we can generate more samples of $\mathbf{y}_{t+1}$ to achieve better approximation. However, since multiple copies of particles are present in (23) due to the resampling operation, approximation described in Algorithm 1 was found to be sufficient for simulations.

D. Extension of the horizon

The considered one-step-ahead optimization can be formally extended to receding horizon optimization. However, the implied computational cost grows exponentially. Future extensions must tackle two problems. First, the particle degeneracy on the horizon. Since integration of the loss functions is based on the empirical approximation, the increase of unknowns further reduces quality of approximation of the integral loss function via importance sampling. More particles is then necessary to preserve accuracy. Second, the number of potential positions of the UAVs grows exponentially. This may be improved by replacing regular grid by random grids, e.g. via particle filtering with good proposal density, [11].

IV. Results

A hypothetical 1 hour long release of radionuclide ^{41}Ar with half-life of decay 109.34 minutes was simulated. Bayesian filtering is performed in time steps $t = 1, \ldots, 18$, with sampling period of 10 minutes. This sampling period was chosen to match the sampling period of the RMN which provides measurements of time integrated dose rate in 10-minute intervals. The same period was assumed for the anemometer. The simulated release started at time $t = 1$ with release activity $Q_i = 1 \times 1e16\, Bq$, $i = 1, \ldots, 6$.

Values of the measurements were simulated as random draws from measurement model (11) with parameters given by the dispersion model with the "true" parameters.

A. Release estimation without UAVs

Particle filter (Section II-E) with $N = 100$ was used to obtain estimates of the posterior. Contours of the expected total dose at time $t = 18$ given observations up to time $t = 18$ are displayed in Figure 4, center-left. Note that the posterior values closely correspond to the simulated values in the part close to the power station. However, with growing distance from the power station the accuracy of estimation of the wind field is deteriorating. This is caused by sparsity of sensors of the RMN. Posterior estimates of the correction coefficient $\theta_{c,t}$ have very high uncertainty and estimation of the bending of the wind field is not possible.

B. Validation of approximations

Quality of approximations of mutual information introduced in Section III-B is now tested experimentally on the results of assimilation. For illustration, the value of mutual information is evaluated for a single UAV in locations on a rectangular grid $a_{1,t} \in \{-1, 0, \ldots, 19\}$km and $a_{2,t} \in \{-1, 0, \ldots, 19\}$km from the power plant. Comparison of the Gaussian approximation (30) with numerical evaluation of (28) using 100 integration points is displayed in Fig. 2. Note that their differences are mainly in scale of the the local maxima, however their locations correspond very well. Since computational requirements
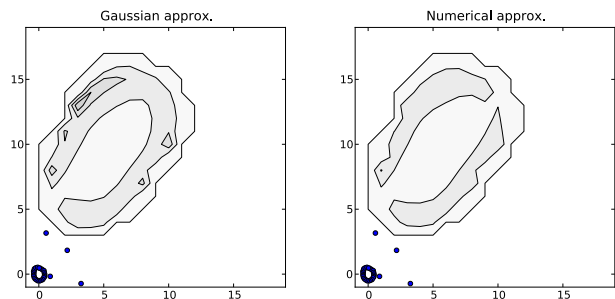

Fig. 2. Contour plot of estimated mutual information on the grid of $\mathbf{a}_t$. **Left**: Gaussian approximation (30); **Right**: numerical integration of (28).
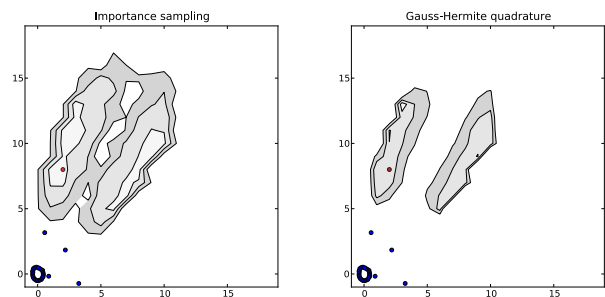

Fig. 3. Comparison of approximations for the misclassification loss at time $t = 11$. **Left**: Importance sampling for a random draw of $\mathbf{x}_{t+1}, \mathbf{y}_{t+1}$, **Right**: Integration using Gauss-Hermite quadrature.

of the Gaussian approximation are significantly lower, it will be used in further experiments.

Similar experiment was performed for methods of evaluation of the miclassification loss function from Section III-C. The main disadvantage of the importance sampling approximation of (22) is its dependence on the realization of the random draws. In Fig. 3, we compare evaluation of the misclassification using the importance sampling and Gauss-Hermite quadrature rules [12]. Note that the results of the importance sampling estimate higher values of the misclassification loss. However, the position of the local minima are in good agreement with the loss evaluated using Gauss-Hermite quadrature rules. Therefore, we will use Algorithm 1 in the following simulations.

C. Navigation of UAVs

The same release of the radioactive material as in Section IV-A was simulated and its estimation was now performed using data from RNM and UAVs that were navigated to minimize the expected loss functions. Results of estimation are compared with the results without UAVs in Figure 4 for both loss functions: mutual information and misclassification count. Note that for both loss functions the UAVs followed the plume and their data allowed to improved estimation of the parameter $\theta_{c,t}$ and thus of the bending of the wind field. However, trajectories of the UAVs differ with the used loss function. Using
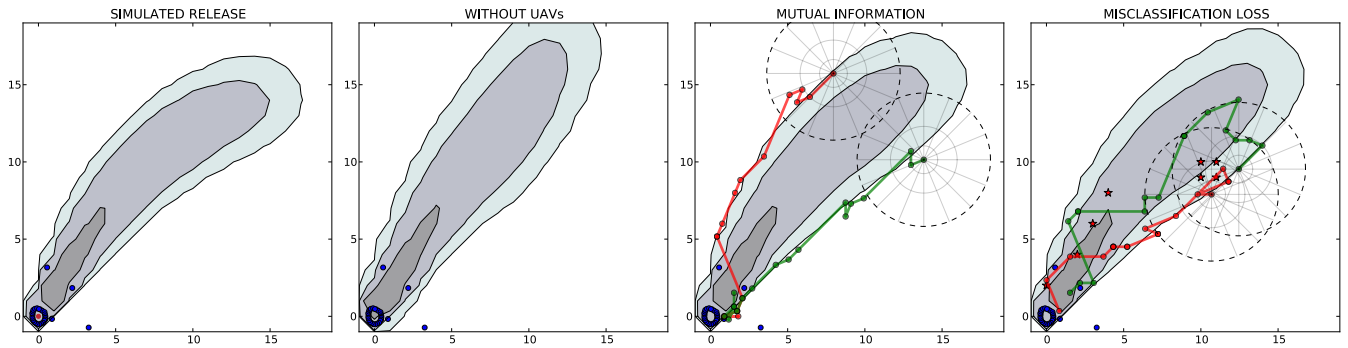
Fig. 4. Results of estimation of the radioactive plume, displayed via contour lines of the true (in case of simulated data) or expected value of the total radiation dose. **Left**: simulated total dose. **Center-left**: estimated dose using RMN only. **Center-right**: estimated dose using RMN+UAVs navigated using mutual information. **Right**: estimated dose using RMN+UAVs navigated using misclassification loss. Position of sensors of the RMN is denoted by blue circles, path of the UAVs by connected circles, and locations of the inhabited areas for the misclassification loss by red stars.
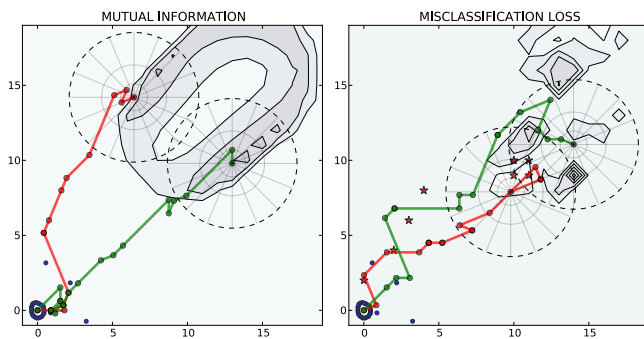

Fig. 5. Illustration of the considered loss functions for a single position of a receptor on a rectangular grid at time $t = 18$.

the mutual information for navigation, the UAVs closely follow contours of the plume. For the misclassification loss, the UAVs navigate closer to the inhabited areas (Figure 4, right, stars). In general, navigation using the misclassification loss is more demanding since it is not as smooth as the mutual information, Figure 5.

V. DISCUSSION AND CONCLUSION

Data acquisition is one of the most important tasks after an accidental release of radioactive material into the atmosphere. Reliable data are necessary for correct assessment of the situation and planning of effective countermeasures. Existing stationary radiation monitoring networks were designed for this purpose, however, they can not be arbitrarily dense. Therefore, the use of mobile measuring devices and unmanned aerial vehicles in particular is a very attractive complement of existing networks. Similarly to the stationary monitoring network, certain level of autonomy is desirable since human supervisors of the power plant will be presumably occupied with an effort to stop the leak rather than observing its consequences. We have shown that current technology allows to design fully autonomous system that is capable to navigate the UAVs such that they maximize

the necessary information about the radioactive release. We have compared two loss functions for navigation of the UAVs. Each has its advantages and disadvantaged for the application domain. Perhaps, a combination of these may be desirable for operational use. However, the presented result already demonstrate the value of automatically navigated UAVs as a complement of the existing stationary radiation protection network.

REFERENCES

[1] G. Heuvelink, Z. Jiang, S. De Bruin, and C. Twenhöfel, "Optimization of mobile radioactivity monitoring networks," *International Journal of Geographical Information Science*, vol. 24, no. 3, pp. 365–382, 2010.

[2] R. Abida and M. Bocquet, "Targeting of observations for accidental atmospheric release monitoring," *Atmospheric Environment*, vol. 43, no. 40, pp. 6312–6327, 2009.

[3] P. Skoglar, "Planning methods for aerial exploration and ground target tracking," 2009.

[4] G. Hoffmann and C. Tomlin, "Mobile sensor network control using mutual information methods and particle filters," *Automatic Control, IEEE Transactions on*, vol. 55, no. 1, pp. 32–47, 2010.

[5] J. Berger, *Statistical Decision Theory and Bayesian Analysis*. New York: Springer, 1985.

[6] J. Zidek, W. Sun, and N. Le, "Designing and integrating composite networks for monitoring multivariate gaussian pollution fields," *Journal of the Royal Statistical Society: Series C (Applied Statistics)*, vol. 49, no. 1, pp. 63–79, 2000.

[7] S. Thykier-Nielsen, S. Deme, and T. Mikkelsen, "Description of the atmospheric dispersion module RIMPUFF," tech. rep., Riso National Laboratory, 1999.

[8] S. Raza, R. Avila, and J. Cervantes, "A 3-D Lagrangian (Monte Carlo) method for direct plume gamma dose rate calculations," *Journal of Nuclear Science and Technology*, vol. 38, no. 4, pp. 254–260, 2001.

[9] W. Caselton and T. Husain, "Hydrologic networks: Information transmission," *Journal of the Water Resources Planning and Management Division*, vol. 106, no. 2, pp. 503–520, 1980.

[10] A. Doucet, N. de Freitas, and N. Gordon, eds., *Sequential Monte Carlo Methods in Practice*. Springer, 2001.

[11] D. Stahl and J. Hauth, "Pf-mpc: Particle filter-model predictive control," *Systems & Control Letters*, 2011.

[12] M. Abramowitz and I. Stegun, *Handbook of Mathematical Functions*. New York: Dover Publications, 1972.